Protein Science (1993), *2*, 1756–1764. Cambridge University Press. Printed in the USA.

Identification of cysteine ligands in metalloproteins using optical and NMR spectroscopy: Cadmium-substituted rubredoxin as a model $[Cd(CysS)_4]^{2-}$ center

COLIN J. HENEHAN,[1,3] DEAN L. POUNTNEY,[1] OLIVER ZERBE,[2] AND MILAN VAŠÁK[1]

[1] Biochemisches Institut and [2] Institut für Organische Chemie der Universität Zürich, Zürich, Switzerland

(RECEIVED June 4, 1993; ACCEPTED July 22, 1993)

Abstract

Optical and NMR methods are presented for the identification of cysteine ligands in Cd-substituted metalloproteins, in particular those containing zinc-fingerlike motifs, using Cd-substituted *Desulfovibrio gigas* rubredoxin (Cd-Rd) as a model $[Cd(CysS)_4]^{2-}$ complex. The ^{113}Cd NMR spectrum of Cd-Rd contains a single ^{113}Cd resonance with a chemical shift position (723.6 ppm) consistent with tetrathiolate metal coordination. The proton chemical shifts of the four cysteine ligands were obtained from one-dimensional heteronuclear (^1H-^{113}Cd) multiple quantum coherence (HMQC) and total coherence spectroscopy (TOCSY)-relayed HMQC experiments. In addition, sequential assignments were made for two short cysteine-containing stretches of the polypeptide chain using a combination of homonuclear proton correlated spectroscopy, TOCSY, and nuclear Overhauser effect spectroscopy experiments, enabling sequence-specific heteronuclear $^3J(^1H^{\beta}$-$^{113}Cd)$ coupling constants for each cysteine to be determined. The magnitude of these couplings (0–38 Hz) follows a Karplus-like dependence with respect to the H^{β}-C^{β}-S^{γ}-Cd dihedral angles, inferred from the crystal structure of the native protein. The difference absorption envelope (Cd-Rd vs. apo-Rd) reveals three distinct transitions with Gaussian-resolved maxima located at 213, 229, and 245 nm, which are paralleled by dichroic features in the corresponding difference CD and magnetic CD spectra. Based on the optical electronegativity theory of Jørgensen, the lowest energy transition has been attributed to a CysS-Cd(II) charge-transfer excitation (ϵ_{245}, 26,000 M^{-1} cm^{-1}) with a molar extinction coefficient per cysteine of 6,500 M^{-1} cm^{-1}. It is proposed that the intensity of this band can be used as a sensitive measure of the number of cysteine ligands present in $Cd(CysS)_{4-n}X_n$ centers.

Keywords: cadmium-substituted rubredoxin; cadmium substitution; cadmium-thiolate charge-transfer bands; cysteine ligation; electronic spectroscopy; NMR; zinc-finger proteins

Recently, a large number of proteins have been found that exhibit metal-dependent transcription regulation activities and contain cysteine-rich sequence motifs capable of coordinating Zn(II) ions (Berg, 1990). Many of these so-called "zinc fingers" are characterized by mononuclear tetrahedral Zn centers with the general formula $[Zn(Cys)_{4-n}(His)_n]$, where $n = 0$–2. In the absence of three-dimensional structures of many such proteins, information about the type of center present would be desirable. Because zinc ions are spectroscopically silent, it has often been necessary to isostructurally substitute it by other metals, such as cadmium or cobalt. The NMR-active isotope of cadmium, ^{113}Cd, has frequently been used to probe the ligand environment of metal-binding sites. However, the interpretation of ^{113}Cd chemical shift in terms of metal ligation alone is complicated by several factors, such as geometric distortion, ligand charge, and coordination number (Summers, 1988). Previously, (^1H-^{113}Cd) correlation experiments using two-dimensional (2D) heteronuclear multiple quantum coherence (HMQC) have been carried out to provide more definitive information about metal ligation in several Cd-substituted metalloproteins (Frey et al., 1985; Live et al., 1985a,b; Otvos et al., 1985; Blake et al., 1992). This approach, however, requires millimolar protein concentrations and substantial amounts of NMR time, limiting the general applicability of this method. A more sensitive and available technique,

Reprint requests to: Milan Vašák, Biochemisches Institut der Universität Zürich, Winterthurerstrasse 190, 8057 Zürich, Switzerland.

[3] Present address: Biotechnology, K-681.4.07, CIBA AG, 4002 Basel, Switzerland.

such as electronic absorption spectroscopy, would therefore be of considerable practical use. It is well documented for Co(II)-substituted metalloproteins that the intensity of the lowest energy CysS-Co(II) ligand-to-metal charge-transfer (LMCT) absorption feature can give quantitative information about the number of metal-thiolate coordination bonds (Holmquist & Vallee, 1979). In principle, the intensity of a CysS-Cd(II) charge-transfer chromophore could also give information relating to the number of thiolate ligands per metal ion. The binding of cadmium to thiolate generates intense absorption bands in the near-UV region. These metal-induced features have been observed previously in a number of Cd-substituted metalloproteins where such thiolate coordination exists, e.g., metallothionein, liver alcohol dehydrogenase (LADH), GAL4 protein, etc. (Kägi & Vallee, 1961; Sytkowski & Vallee, 1979; Basile & Coleman, 1992). However, no attempt has been made to use these features quantitatively.

In the present work, we have isostructurally replaced the native Fe(III) ion in the crystallographically defined $Fe(CysS)_4$ center in rubredoxin from *Desulfovibrio gigas* with $^{113}Cd(II)$ ion and investigated its NMR and optical properties as a model $[Cd(CysS)_4]^{2-}$ complex. Using one-dimensional (^1H-^{113}Cd) HMQC and total coherence spectroscopy (TOCSY)-relayed HMQC experiments, all proton chemical shifts of the cysteine ligands could be obtained. Thus, in combination, these two straightforward experiments permitted the type and number of metal-coordinating spin systems to be deduced. In addition, the amino acid sequence positions of the Cys ligands were obtained through a combination of homonuclear proton correlated spectroscopy (COSY), TOCSY, and nuclear Overhauser effect spectroscopy (NOESY) experiments. The magnitudes of the heteronuclear $^3J(^1H^\beta$-$^{113}Cd)$ coupling constants for all four cysteines appear to follow a Karplus-like dependence with respect to the H^β-C^β-S^γ--Cd dihedral angles, inferred from the crystal structure of the native protein. Secondly, from the analysis of difference electronic absorption, CD, and magnetic CD (MCD) spectra, the position of the lowest energy electronic transition has been determined. Based on Jørgensen's theory of optical electronegativity (Jørgensen, 1970), this band is assigned to a CysS-Cd(II) charge-transfer transition. We propose that the molar extinction coefficient per cysteine thiolate obtained for this band may be used in the quantification of cysteine ligands in Cd-substituted zinc-fingerlike proteins.

Results

Physical characterization of Cd(II)-reconstituted rubredoxin

The iron ion of native rubredoxin (Fe(III)-Rd) has been replaced by the diamagnetic Cd(II) ion. A molar extinction coefficient (ϵ) at 280 nm of 9,000 $M^{-1}\,cm^{-1}$ was determined for the apoprotein, and that of the Cd-Rd derivative was found to be slightly greater, at 11,500 $M^{-1}\,cm^{-1}$. In the case of the apoprotein, the value agrees quite well with that obtained when the extinction coefficients of the individual isolated chromophores contributing to the 280-nm absorbance are summed (ϵ_{sum}, 9,200 $M^{-1}\,cm^{-1}$). Metal determination by atomic absorption spectroscopy yielded 1.02 mol of Cd/mol of Rd. This form eluted in gel filtration chromatography (Superdex 75 column) with an apparent molecular weight of ~6,000 Da, similar to that of the native Fe protein (data not shown).

Spectroscopic characterization of Cd(II)-Rd

NMR properties

The ^{113}Cd NMR spectrum of ^{113}Cd-Rd exhibits a single resonance at 723.6 ppm (half-width 25 Hz) (data not shown). The chemical shift position of this resonance is in line with those observed in other tetrahedral tetrathiolate cadmium sites (610–750 ppm) (Summers, 1988). From (^1H-^{113}Cd) HMQC experiments, the proton chemical shifts of the corresponding metal ligands were obtained. Because only one Cd(II) ion is bound to the protein, a one-dimensional (1D) approach could be employed, facilitating the rapid accumulation (1 h each) of a series of high-quality spectra with defocussing and refocussing delay times of 80 to 2 ms, reflecting heteronuclear couplings between 6 and 250 Hz, respectively (data not shown). Representative 1D ^{113}Cd-filtered proton spectra in the spectral region corresponding to cysteine H^β resonances (between 2.5 and 4.0 ppm) are shown in Figure 1B and C. Protons with very small heteronuclear (^1H-^{113}Cd) couplings may escape detection due to inefficient transfer of coherence during the filtering process. Thus, in order to obtain proton chemical shifts of the entire cysteine spin systems, an independent experiment was performed in which the HMQC pulse sequence was extended with a TOCSY relay (see Fig. 8C and Materials and methods). In this 1D experiment, even the cysteine amide protons were detected by multiple relay via the C^β protons (data not shown). The corresponding 1D HMQC–TOCSY spectrum between 2.5 and 4.0 ppm reveals two additional H^β peaks (Fig. 1A). The TOCSY relay experiment led to the observation of signals corresponding to $H^{\beta a}$ of Cys 39 and $H^{\beta b}$ of Cys 6, which would otherwise have remained undetected (see below).

That the proton signals in the ^{113}Cd-filtered spectra originate from the C^β protons of Cys residues has been established unambiguously by the sequence-specific assignment of these resonances. The following targeted strategy was adopted for the complete sequential assignment of the two cysteine-containing stretches encompassing residues 5–11 and 37–44, respectively (Fig. 2). Spin system identifications were made using standard double-quantum filtered (2QF) COSY and TOCSY methodology

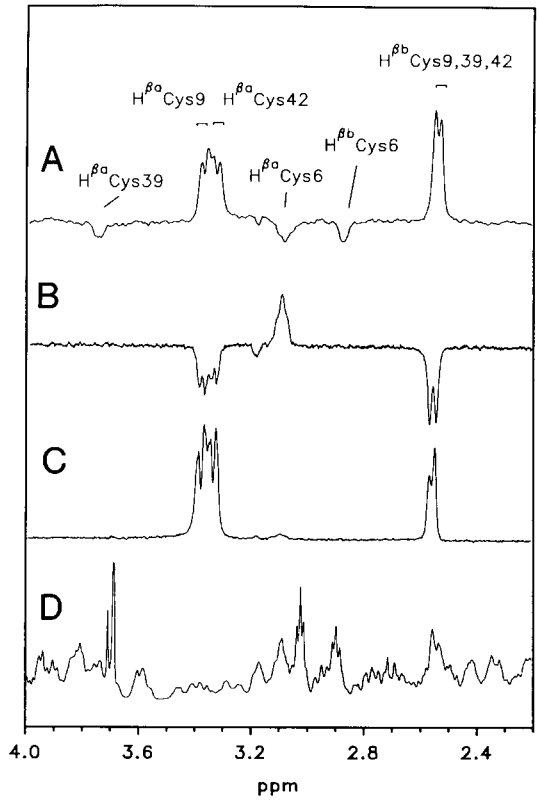

Fig. 1. Region of the 600-MHz ^{113}Cd-decoupled heteronuclear (^{1}H-^{113}Cd) correlation spectra of ^{113}Cd-Rd containing the H^{β} resonances of cysteines using the pulse sequences in Figure 8. **A:** 1D (^{1}H-^{113}Cd) HMQC-TOCSY spectrum optimized for a (^{1}H-^{113}Cd) scalar coupling of 12.5 Hz, extended with a 40-ms ^{1}H TOCSY relay (see Fig. 8C for pulse sequence). **B, C:** 1D (^{1}H-^{113}Cd) HMQC spectra recorded using the pulse sequence shown in Figure 8B with defocussing and refocussing delays of 40 and 10 ms, reflecting approximate heteronuclear (^{1}H-^{113}Cd) coupling constants of 12.5 and 50 Hz, respectively. **D:** Reference proton spectrum over the same region. All spectra were recorded at 27 °C. Cysteine resonances are identified with their sequence-specific assignments, where $H^{\beta a}$ and $H^{\beta b}$ indicate H^{β} resonances with larger and smaller ^{1}H chemical shifts, respectively (see Table 1). The resonance splittings due to resolved homonuclear proton couplings are indicated with solid brackets.

and sequential assignments were obtained from NOESY experiments (Wüthrich, 1986). In general, the spin systems in the TOCSY spectrum of Cd-Rd were best separated in the amide region. Only Cys 9 and Cys 42, which form a part of two Val-Cys-Gly tripeptide sequences, have a Gly residue at the $n + 1$ position (Fig. 2). Initially, the proton chemical shift positions of all five Gly residues were identified from their unique appearance in the H^{α}-NH region of the triple-quantum filtered (3QF) COSY spectrum. Secondly, the A_3B_3MX spin systems of the three Val residues were identified based on their characteristic pattern of cross peaks in the TOCSY spectrum. Using sequential NH-NH connectivities, the two Val-Cys-Gly tripeptide sequences were then assigned. Further identification of short-range through-space connectivities to the adjacent Tyr 11 and Ala 44 residues established the sequence-specific assignment of Cys 9 and Cys 42, respectively (Table 1; Fig. 2). The remaining two Cys residues, Cys 39 and Cys 6, are part of two unique tripeptides, Trp-Ala-Cys and Val-Cys-Thr, respectively (Fig. 2). The sequential assignment of the Trp-Ala-Cys tripeptide containing Cys 39 was aided by the recognition of the single Trp 37 by a distinct indole ring proton resonance at 10.8 ppm (Fig. 2) and the observation of long-range NOEs between Trp 37 and Cys 39. In the Val-Cys-Thr tripeptide, Cys 6 is flanked by Val 5 and Thr 7 in the amino acid sequence. The latter spin systems were identified and the tripeptide assigned (Table 1; Fig. 2). Subsequently, the whole peptide segment between residues Val 5 and Tyr 11 could be sequentially traced through using NH-NH and NH-H^{α} through-space connectivities (Table 1; Fig. 2).

The magnitudes of the $^{3}J(^{1}H^{\beta}$-$^{113}Cd)$ coupling constants of all four cysteines were estimated either from the 2QF COSY or the 1D (^{1}H-^{113}Cd) HMQC spectra. The large heteronuclear $^{3}J(^{1}H^{\beta}$-$^{113}Cd)$ coupling constants of Cys 9 and Cys 42 were extracted from the ($H^{\beta a}$, $H^{\beta b}$) cross peaks in the 2QF COSY spectra obtained with and without ^{113}Cd decoupling, as illustrated in Figure 3. Both Cys 6 and Cys 39 exhibit small heteronuclear $^{3}J(^{1}H^{\beta}$-$^{113}Cd)$ coupling constants (<5 Hz) that are unresolved in the 2QF COSY cross-peak patterns. For Cys 6, their magnitudes were estimated from a comparison of the 1D (^{1}H-^{113}Cd) HMQC spectra, obtained with and without ^{113}Cd decoupling, assuming Lorentzian line shapes (data not shown). Because the $H^{\beta b}$ resonance of Cys 39 is degenerate with $H^{\beta b}$ resonances of Cys 9 and Cys 42, the latter approach could not be applied (Table 1). However, assuming that a similar $H^{\beta a}$-$H^{\beta b}$ geminal coupling exists for Cys 39 and Cys 6, the magnitude of the $^{3}J(^{1}H^{\beta b}$-$^{113}Cd)$ coupling was

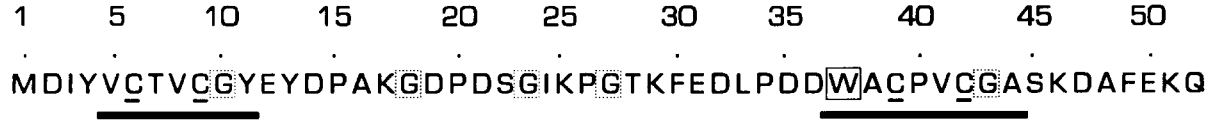

Fig. 2. Amino acid sequence of *Desulfovibrio gigas* rubredoxin using standard single-letter code (Bruschi, 1976). The five glycine residues are highlighted in dotted boxes and the single tryptophan is indicated by a solid box. Metal-coordinating cysteine residues are underlined. The solid horizontal bars identify the two cysteine-containing stretches of the polypeptide chain for which sequential assignments of ^{1}H resonances were obtained.

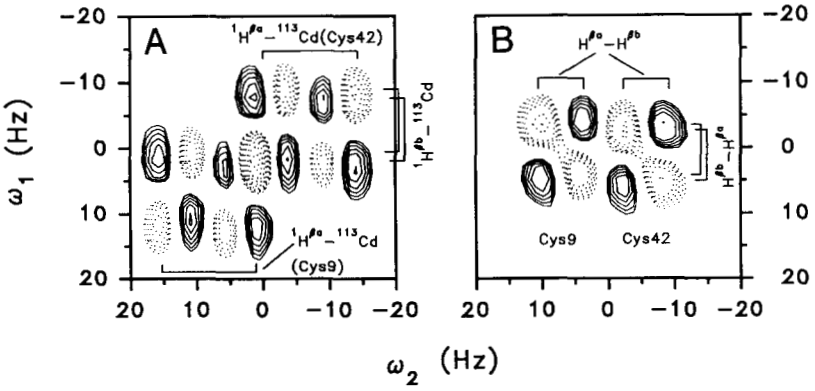

Fig. 3. Expansion of the 600-MHz ^1H 2QF COSY spectrum of ^{113}Cd-Rd showing the ($H^{\beta a}$-$H^{\beta b}$) cross peaks of Cys 9 and Cys 42 without (**A**) and with (**B**) ^{113}Cd decoupling of the proton resonances. Spectra were recorded at 27 °C. Negative levels are indicated by dotted lines. The heteronuclear $^3J(^1H^{\beta a,b}$-$^{113}Cd)$ couplings are shown by solid brackets (see Table 1).

estimated based on the intensity of the $H^{\beta a}$ TOCSY relay signal of Cys 39 compared to that of Cys 6 (Fig. 1A; Table 1). The proton chemical shifts and $^3J(^1H^{\beta}$-$^{113}Cd)$ coupling constants obtained for each of the four cysteine ligands in Cd-substituted *D. gigas* rubredoxin are summarized in Table 1. The positions of the cysteine $^1H^{\beta}$ resonances are similar to those reported for the zinc-substituted rubredoxin from the hyperthermophilic bacterium *Pyrococcus furiosus* (RdPf) (σ, 0.18 ppm) (Blake et al., 1991).

Optical properties

In order to examine the effect of metal ions on the secondary structure of the apoprotein (apo-Rd), the far-UV CD spectrum (between 260 and 180 nm) of this form was compared with that of native Fe(III)-Rd and of reconstituted Cd-Rd (Fig. 4). The CD spectra of both the native protein and the apoprotein are characterized by two negative bands at 225 and 201 nm and a positive band at 195 nm arising from the protein amide transitions. The close similarity in both CD spectra indicates that the protein structure is unaffected by removal of the bound metal ion. Moreover, there are no optically active CysS-Fe(III) charge-transfer transitions manifested in this spectral region. In contrast, the binding of Cd(II) ions to apo-Rd introduces metal-dependent changes above 200 nm in the CD spectrum (Fig. 4), as well as in the absorption and MCD spectra (Fig. 5A,C, respectively). However, the high-energy CD features of Cd-Rd and native Fe-Rd below 200 nm are essentially unchanged. Because this spectral region is particularly sensitive to changes in protein secondary structure, this result suggests that the overall protein fold of Cd-Rd is unaltered on metal binding. At this point it should be noted that the presence of strong metal-induced features in the region of the CD spectrum (below 250 nm) usually used in protein secondary structure analysis precludes the use of this technique in proteins containing the CysS-Cd(II) chromophore.

The electronic absorption, CD, and MCD spectra of apo-Rd and Cd(II)-Rd above 190 nm are shown in Figure 5. The binding of Cd(II) ions to apo-Rd introduces a broad feature between 200 and 260 nm superimposed on the absorption envelope of the apoprotein (Fig. 5A). At the pH used (pH <6.5), no contribution to the apo-

Table 1. *Cysteine ^1H chemical shifts and $^3J(^1H^{\beta}$-$^{113}Cd)$ coupling constants for Cd-substituted Desulfovibrio gigas rubredoxin*

	Chemical shift (ppm)				$^3J(^1H$-$^{113}Cd)$ (Hz)[a]	
Residue	NH	H^{α}	$H^{\beta a}$	$H^{\beta b}$	$H^{\beta a}$	$H^{\beta b}$
Cys 6	8.14	5.31	3.11	2.91	3.0 ± 1.0	0.5 ± 0.5[b]
Cys 9	8.76	5.10	3.37	2.56	38.0 ± 1.5	17.0 ± 1.5
Cys 39	8.22	5.35	3.75	2.55	0.5 ± 0.5[b]	2.5 ± 1.0
Cys 42	8.43	5.00	3.30	2.56	37.0 ± 1.5	18.0 ± 1.5

[a] Estimated errors are indicated in Hz.
[b] Unresolved coupling.

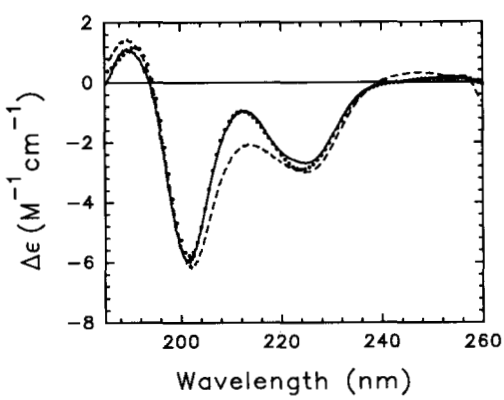

Fig. 4. Far-UV CD spectra of native Fe(III) (solid line), apo- (dotted line), and Cd(II)-substituted (dashed line) rubredoxin from *Desulfovibrio gigas*. Spectra are the average of four accumulations recorded at 1 nm min^{-1} with a time constant of 16 s. Protein concentrations were between 25 and 50 μM and the cuvette pathlength was 0.02 cm. For details see Materials and methods.

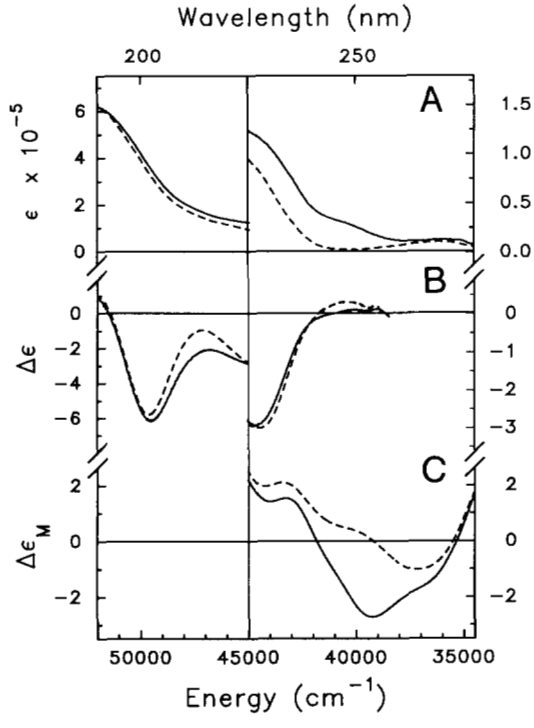

Fig. 5. Electronic absorption (**A**), CD (**B**), and MCD (**C**) spectra of apo- (dashed lines) and Cd-Rd (solid lines). Protein concentrations and cell pathlengths used in the absorption and MCD measurements were 10 μM (1 mm) and 40 μM (2 mm), respectively. Conditions for the CD spectra are as in Figure 4. For details see Materials and methods.

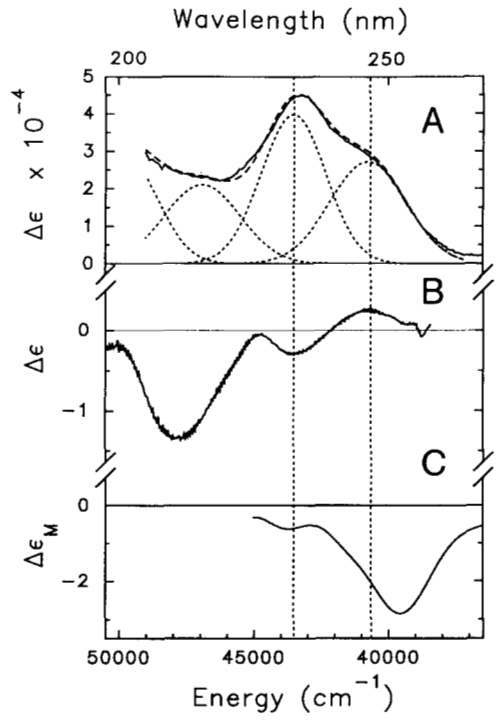

Fig. 6. Difference electronic absorption (solid line) (**A**), CD (**B**), and MCD (**C**) spectra of Cd-Rd vs. apo-Rd generated using the spectra shown in Figure 5. The results of the Gaussian analysis of the difference absorption envelope are illustrated in A. Individual component bands are shown as short dashes and the overall fit as long dashes.

Rd spectrum above 205 nm from deprotonated cysteine residues (pK_a ~8.5) is expected. The shoulders on the low-energy side of the 280-nm band, due to the single tryptophan residue, are less pronounced in apo-Rd than in either Cd-Rd (Fig. 5A) or native Fe(III)-Rd (Moura et al., 1977). The sharpening of these features can be attributed to metal binding close to the indole ring and presumably reflects the similarity in the metal ion environments of the two metal-containing forms. The absorption features introduced by cadmium binding are also reflected in the corresponding CD and MCD spectra (Fig. 5B,C). However, more information concerning the origin of these bands may be obtained by analyzing the corresponding difference spectra, i.e., Cd-Rd vs. apo-Rd. Note that no major structural changes accompanying Cd binding to apo-Rd occur (see above).

The difference absorption, CD, and MCD spectra (Cd-Rd vs. apo-Rd) are shown in Figure 6. The metal-induced absorption envelope, centered at 232 nm, can be resolved into three Gaussian bands located at 245, 229, and 213 nm (Fig. 6A). Dichroic features in similar positions are also observed in the corresponding CD spectrum (Fig. 6B). The low-energy region (above 235 nm) of the difference MCD spectrum exhibits an extremum at (−)254 nm, which is substantially red shifted from the lowest energy absorption or CD bands (Fig. 6C). In tetrahedral halide (Gunter et al., 1975) and thiolate (Carson et al., 1981) model complexes with divalent d^{10} metal ions, T_d symmetry gives rise to a derivative-shaped MCD profile with an inflection point at the absorption maximum, i.e., an MCD A-term. By analogy with these studies, we propose that the (−)254-nm MCD band is the negative lobe of an A-term arising from the transition at 245 nm.

In transition and post-transition metal complexes, the energy of the first (lowest energy) charge-transfer transition may be calculated using the semiempirical optical electronegativity concept of Jørgensen (1970). According to this theory, the position of the first (lowest energy) allowed absorption band ($\bar{\nu}$, expressed in cm^{-1}) is given by the following simple expression:

$$\bar{\nu} = 30{,}000[\chi_{opt}(L) - \chi_{opt}(M)], \qquad (1)$$

where $\chi_{opt}(L)$ and $\chi_{opt}(M)$ are the optical electronegativities of the ligand (L) and the metal (M), respectively. Based on a correlation with the position of the first absorption bands in d^{10} metal–tetrahalide complexes of Zn(II), Cd(II), and Hg(II) ions, a value of 1.26 for the optical electronegativity of Cd, χ_{opt}(Cd), has been derived (Vašák et al., 1981). Substituting the energy of the first resolved band of Cd-Rd, $\bar{\nu}$ at 40,800 cm^{-1}

(ϵ = 26,000 M^{-1} cm^{-1}), together with the value for χ_{opt}(Cd) in Equation 1, a value of 2.62 for χ_{opt} of cysteine sulfur is obtained. This calculated value is in good agreement with that of 2.6 estimated previously (McMillin, 1978). Hence, we attribute the first metal-induced transition in Cd-Rd to the lowest energy CysS-Cd(II) LMCT band. Although further work is required to definitively assign the remaining two bands, it is clear that they are predominantly charge-transfer in character.

Discussion

The order of affinity of metals for cysteine sulfur follows the order found in model thiolate complexes, i.e., Zn(II) < Cd(II) < Hg(II). Therefore, Cd may compete with and displace Zn in kinetically labile cysteine-containing metal sites, such as those found in a number of DNA-binding proteins. For example, Cd derivatives of the TAT protein from human immunodeficiency virus (Frankel et al., 1988) and the DNA-binding domain of the human glucocorticoid receptor (Pan et al., 1990) have been prepared by incubation of the zinc proteins with cadmium salt. In the present study, the optical and NMR characterization of Cd-substituted rubredoxin allows a number of general points to be made concerning the use of Cd as a probe for the structure of metal-binding sites in proteins. Particularly, we have sought to examine the possibility of obtaining useful information about the number of cysteine ligands present in zinc-fingerlike proteins when the quantity of biological material available is insufficient to permit more detailed structural studies. Furthermore, proteins containing zinc-fingerlike domains are often too large to allow their complete three-dimensional structures to be solved by NMR methods.

In this work, 1D (^{1}H-^{113}Cd) HMQC and HMQC-TOCSY spectroscopy, in combination with conventional 2D COSY, TOCSY, and NOESY methods, have been used to assign Cd-binding residues and to estimate $^3J(^1H\text{-}^{113}Cd)$ heteronuclear coupling constants. Previously, 2D (^{1}H-^{15}N) HMQC-TOCSY experiments analogous to the 1D approach taken here have been applied in the spin-system identification process in proteins, aiding in the resolution of individual amide proton resonances according to their ^{15}N chemical shifts (Gronenborn et al., 1989; Marion et al., 1989). Using a similar 2D approach, only one resolved (^{1}H-^{113}Cd) coupling would be required to obtain proton resonances of the entire spin system of a given metal ligand in a Cd-substituted metalloprotein.

In our NMR studies of Cd-Rd, a variation in the magnitude of the heteronuclear $^3J(^1H^{\beta}\text{-}^{113}Cd)$ coupling constants between approx. 0 and 38 Hz (see Table 1) was observed. Inspection of the tetrahedral tetrathiolate metal-binding site geometry in the X-ray crystal structure of the native iron protein reveals two sets of torsion angles, defined as $C^{\alpha}\text{-}C^{\beta}\text{-}S^{\gamma}\text{-}Fe$, for the four ligated cysteine residues. One set (Cys 6 and Cys 39) has torsion angles of −172 and −178°, respectively, and the other (Cys 9 and Cys 42), −91 and −94°, respectively (Frey et al., 1987). Thus, the C^{α} conformations of Cys 6 and Cys 39 are *anti* and those of Cys 9 and Cys 42 are *gauche* with respect to the central metal ion (see Fig. 7A). Assuming tetrahedral geometry about the cysteine β carbons, the corresponding $H^{\beta}\text{-}C^{\beta}\text{-}S^{\gamma}\text{-}Fe$ dihedral angles (ϕ_a, ϕ_b) for the two β protons can be derived. In many systems, the magnitude of the ^{3}J coupling is proportional to $\cos^2\phi$ (Karplus, 1959). Thus, assuming the geometry of the metal center is unchanged in the Cd derivative, four small and four large vicinal $^1H^{\beta}\text{-}^{113}Cd$ couplings would be expected. The pattern of cysteine $^3J(^1H^{\beta}\text{-}^{113}Cd)$ coupling constants observed is consistent with this proposal (see Table 1). For homonuclear $^3J(^1H\text{-}^1H)$ couplings (Karplus, 1959) and heteronuclear $^3J(^1H\text{-}^{15}N)$ and $^3J(^1H\text{-}^{13}C)$ couplings (Bystrov, 1976), Karplus-type relationships, which correlate the size of the vicinal coupling constant with the dihedral angle, have been established. At present, no such correlation has been made for systems contain-

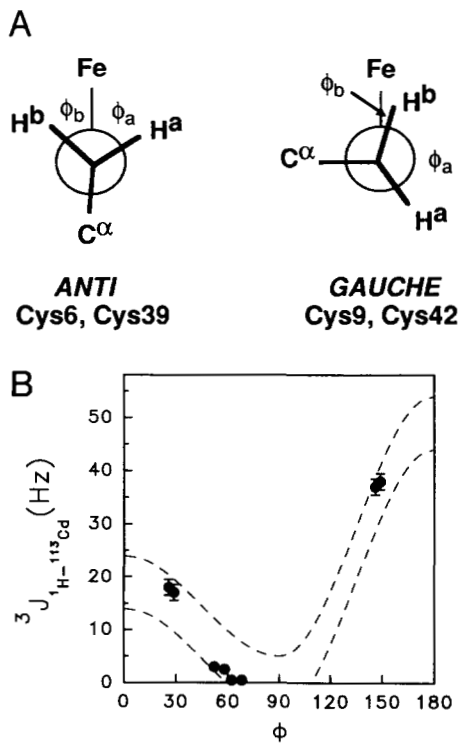

Fig. 7. A: Newman projection representing the $H^{\beta a,b}\text{-}C^{\beta}\text{-}S^{\gamma}\text{-}Fe$ dihedral angles (ϕ_a, ϕ_b) in the the $Fe(CysS)_4$ site of *Desulfovibrio gigas* rubredoxin, showing both *anti* and *gauche* conformations. **B:** Magnitude of the $^3J(^1H\text{-}^{113}Cd)$ coupling constant for cysteine β protons in the $Cd(CysS)_4$ center of Cd(II)-substituted *D. gigas* rubredoxin vs. the dihedral angle, ϕ, deduced from the crystal structure of the native Fe(III) protein (see Table 1 and Discussion). Dashed lines illustrate plots of the Karplus relationship, $J = b(\cos^2\phi) - a$, where b = 19 Hz when $0° \leq \phi \leq 90°$, b = 49 Hz when $90° \leq \phi \leq 180°$, and $a = \pm 5$ Hz.

ing heavier elements such as sulfur and cadmium.[1] In Figure 7B, the magnitudes of the $^3J(^1H^{\beta a,b}\text{-}^{113}Cd)$ coupling constants of cysteines in Cd-Rd are plotted against the $H^{\beta}\text{-}C^{\beta}\text{-}S^{\gamma}\text{-}Cd$ dihedral angles (ϕ_a, ϕ_b) derived from the X-ray structure of the native protein. Excepting the limited number of data points available, the variation in heteronuclear couplings observed resembles a Karplus-like dependence. Clearly, a definitive relationship of this kind would be of great use in the structural investigation of Cd-substituted metalloproteins by NMR and will be the subject of further study.

The binding of Cd(II) ions to apo-Rd induces absorption, CD, and MCD spectral features characteristic of the metal and the coordinating ligands. Gaussian analysis of the difference absorption profile reveals three bands, indicating the presence of at least three metal-induced transitions. This is supported by the presence of bands in similar positions in the corresponding CD spectrum. The position of the lowest energy transition was found to be in good agreement with that predicted from Jørgensen's concept of optical electronegativity, identifying it as a CysS-Cd(II) LMCT transition.

An absorption profile similar to that of Cd-Rd has also been observed for a number of other Cd-substituted metalloproteins, in which thiolate ligation occurs in both mononuclear and clustered arrangements (see Table 2). It has been shown that, for Co(II)-substituted metalloproteins, the intensity of the lowest energy CysS-Co(II) LMCT absorption features can provide quantitative information about the number of metal-thiolate coordination bonds (Holmquist & Vallee, 1979). Similarly, the intensity of the CysS-Cd(II) charge-transfer chromophore should be proportional to the number of CysS-Cd coordination bonds. The molar extinction coefficient of the first Gaussian-resolved band at 245 nm in Cd-Rd is 26,000 M^{-1} cm^{-1}, making the contribution from each cysteine thiolate 6,500 M^{-1} cm^{-1}. A similar value of 6,000 M^{-1} cm^{-1} per thiolate has been reported for Cd_7-metallothionein, which exhibits a Cd-induced shoulder at 249 nm with $\epsilon = 120{,}000$ M^{-1} cm^{-1} (Willner et al., 1987). In this structurally well-defined protein, 20 cysteine thiolates are involved in the binding of seven Cd(II) ions (Braun et al., 1992). Moreover, a pronounced shoulder at 243 nm ($\epsilon \approx 5{,}500$ M^{-1} cm^{-1}) has been reported in the difference absorption spectrum of Cd-substituted S-100b protein, which contains a single cysteine ligand in the Cd-binding site (Donato et al., 1991). These findings confirm that the intensity of the lowest energy CysS-Cd(II) LMCT band is proportional to the number of cysteine thiolate ligands involved in metal binding. Therefore, we propose that, based on a molar extinction coefficient of about 6,000 M^{-1} cm^{-1} per cysteine thiolate, the number of cysteines involved in metal binding in a given Cd-substituted metalloprotein can be estimated using difference absorption spectroscopy. Because of the greater sensitivity of electronic spectroscopy compared to that of NMR spectroscopy, this optical method may be applied when only very limited quantities of protein are available (i.e., 1×10^{-9} mol Cd vs. 5×10^{-7} mol ^{113}Cd) for NMR.

[1] During the review process of this article, we were informed that a similar Karplus-type relationship has been observed between the $^3J(^1H^{\beta}\text{-}^{199}Hg)$ coupling constants and the $H^{\beta}\text{-}C^{\beta}\text{-}S^{\gamma}\text{-}Hg$ dihedral angles in the $Hg(CysS)_4$ center of ^{199}Hg-substituted rubredoxin from *Pyrococcus furiosus* (Blake et al., 1993).

Table 2. *Energies of CysS-Cd(II) charge-transfer transitions of Cd-substituted metalloproteins*

	Energy (cm^{-1})			Reference
Cd-rubredoxin	46,900	43,700	40,800	Present work
Cd-metallothionein	49,700	43,300	40,000	Vašák et al., 1981
Cd/Zn LADH[a]	–	42,000	39,800	Sytkowski and Vallee, 1979
Cd-GAL4	45,870	42,920	40,000	Basile and Coleman, 1992
Cd-TAT[b]	–	42,300	40,300	Frankel et al., 1988

[a] Estimated from the difference absorption spectrum.
[b] Estimated from the CD spectrum.

Materials and methods

Rubredoxin (Fe(III)-Rd), isolated from the anaerobic bacterium *D. gigas* (N.C.I.B. 9335), was obtained from Dr. M. Bruschi (CRNS, Marseille). Buffers used in the preparation of apo-Rd and Cd(II)-Rd were rendered metal free by treatment with the metal-chelating resin Chelex 100 (Bio-Rad). All chemicals used were reagent grade or better. Protein concentrations used in the determination of molar extinction coefficients of apo-Rd and Cd-Rd were determined by quantitative amino acid analysis using a Chromocon 500 (Kontron Analytical) amino acid analyzer. Values were verified independently using the positive MCD band at 294 nm, due to the protein's single tryptophan, as described (Holmquist & Vallee, 1973).

Apo-Rd was prepared essentially according to published procedures (Moura et al., 1991). Briefly, the holoprotein (8 mg) was precipitated by incubation in 5% trichloroacetic acid (TCA) containing 0.5 M 2-mercaptoethanol at 4 °C for 30 min (total sample volume 1 mL). The precipitated apoprotein was recovered by centrifugation ($10{,}000 \times g$) and was then resuspended in 0.5 M Tris-base containing 0.06 M 2-mercaptoethanol. The precipitation and centrifugation steps were repeated to ensure complete metal removal. Subsequently, the pellet was resuspended in 50 mM Tris-HCl, 0.06 M 2-mercaptoethanol, pH 7.6.

Cadmium reconstitution was carried out by the addition of a 1.4 molar excess of 98% enriched $^{113}CdCl_2$ (Harwell) to the above apo-Rd solution. The sample was then desalted over a Sephadex G-25 column equilibrated with

50 mM Tris-HCl, pH 7.6. In contrast to the native protein, cadmium could subsequently be released from Cd-Rd by acidification with HCl (pH 2). Analytical gel filtration was performed using a Superdex 75 column (1 × 30 cm) (Pharmacia) attached to a Pharmacia/LKB fast performance liquid chromatograph system. The sample was eluted with 50 mM Tris-HCl, 50 mM NaCl, pH 8.6. The column was calibrated with the following molecular weight markers: bovine pancreatic trypsin inhibitor (6,500 Da), ribonuclease A (13,700 Da), myoglobin (17,800 Da), chymotrypsinogen (25,000 Da), and ovalbumin (45,000 Da).

Metal determinations were made using an Instrumentation Laboratory IL 12 atomic absorption spectrometer. Absorption spectra were recorded on a Cary 3 spectrophotometer. A Jasco spectropolarimeter (model J-500C) connected on line with an IBM personal computer was used in all CD and MCD measurements. Samples used for CD spectroscopy were in 50 mM potassium phosphate buffer. A magnetic field of 1.5 *T* was used for MCD studies. Gaussian analysis of the difference electronic absorption spectrum was carried out using the program Peakfit (Jandel Scientific) on an IBM PS/2 computer.

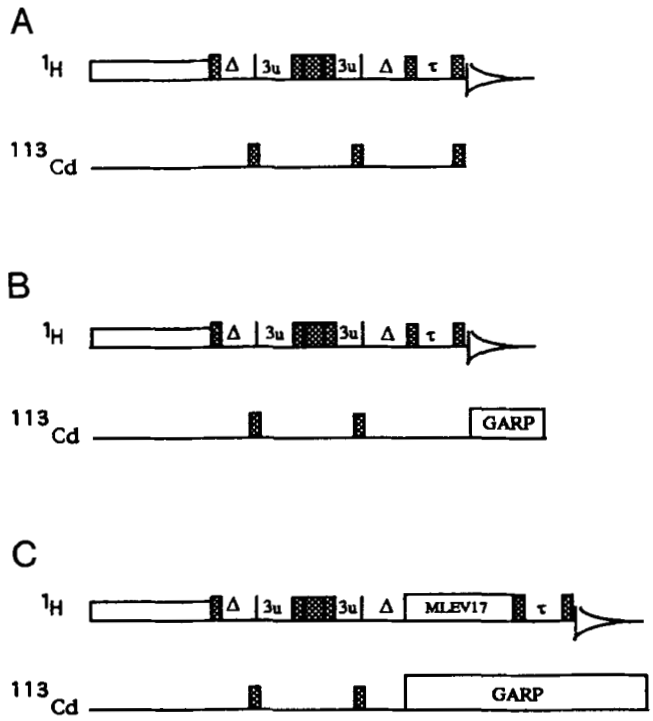

Fig. 8. Pulse sequences used in the heteronuclear 1D (^{1}H-^{113}Cd) correlation experiments shown in Figure 1. **A:** HMQC pulse sequence, including z-filter and purge pulse on the ^{113}Cd channel. **B:** HMQC pulse sequence with the addition of ^{113}Cd decoupling during data acquisition. **C:** ^{113}Cd-decoupled HMQC pulse sequence extended with a subsequent multiple proton relay via an isotropic MLEV17 mixing train, as used in the TOCSY-relayed HMQC experiment (see Fig. 1A). Refocussing and defocussing delays relating to the heteronuclear couplings are marked by Δ.

The ^{1}H and ^{113}Cd NMR spectra were recorded on a Bruker AMX-600 spectrometer. The NMR sample (2 mM protein in 50 mM [$^2H_{11}$]Tris-HCl, 0.1 M NaCl, pH 7.6) in 90% H_2O/10% D_2O (v/v) was measured in a 5-mm-diameter NMR tube. The chemical shift of ^{113}Cd is reported in parts per million (ppm) relative to 0.1 M $^{113}Cd(ClO_4)_2$. In the ^{1}H NMR studies, the chemical shifts are referenced to the 4.80-ppm resonance of H_2O at 27 °C. Homonuclear 2QF COSY, 3QF COSY, TOCSY, and NOESY experiments were performed using standard pulse sequences with solvent suppression being achieved by low-power pre-irradiation. The latter spectra have been acquired at 27 °C with an additional set of COSY and TOCSY spectra obtained at 37 °C. Mixing times of 100 and 200 ms were used in the NOESY measurements. The TOCSY spectra were recorded using an 80-ms MLEV17 spin lock ($\gamma B_z/2\Theta$ approx. 7,500 Hz). The pulse sequences used in the (^{1}H-^{113}Cd) HMQC experiments are illustrated in Figure 8. Pulse sequences A and B, used to obtain the chemical shifts of ^{113}Cd-coupled protons, are essentially identical to those published by Frey et al. (1985) for metallothioneins. Sequence B includes ^{113}Cd decoupling during data acquisition (see Fig. 1B,C). Sequence C contains the TOCSY relay extension aiding in the identification of ^{113}Cd-coupled spin systems, i.e., cysteine ligands (see Fig. 1A). All spectra were measured in phase-sensitive mode with data matrices of 2,048 × 512 time domain data points. Data processing was done with single zero-filling, and the data were apodized using a cosine-bell window function.

Acknowledgments

We acknowledge J.H.R. Kägi and W. von Philipsborn for helpful discussions. This work was supported in part by grants in aid from the Schweizerischer Nationalfonds (31-25655.88 and 31-32572.91), Geigy-Jubiläums-Stiftung, and Stiftung für wissenschaftliche Forschung an der Universität Zürich.

References

Basile, L.A. & Coleman, J.E. (1992). Optical activity associated with the sulfur to metal charge transfer bands of Zn and Cd GAL4. *Protein Sci. 1*, 617–624.

Berg, J.M. (1990). Zinc finger domains: Hypotheses and current knowledge. *Annu. Rev. Biophys. Biophys. Chem. 19*, 405–421.

Blake, P.R., Lee, B., Park, J.-B., Zhou, Z.H., Adams, M.W.W., & Summers, M.F. (1993). Heteronuclear magnetic resonance studies of Zn, ^{113}Cd, and ^{199}Hg substituted *P. furiosus* rubredoxin: Implications for biological electron transfer. *New J. Chem.*, in press.

Blake, P.R., Lee, B., Summers, M.F., Adams, M.W.W., Park, J.-B., Zhou, Z.H., & Bax, A. (1992). Quantitative measurement of small through-hydrogen-bond and "through-space" ^{1}H-^{113}Cd and ^{1}H-^{199}Hg J couplings in metal substituted rubredoxin from *Pyrococcus furiosus*. *J. Biomol. NMR 2*, 527–533.

Blake, P.R., Park, J.-B., Bryant, F.O., Aono, S., Magnuson, J.K., Eccleston, E., Howard, J.B., Summers, M.F., & Adams, W.W. (1991). Determinants of protein hyperthermostability: Purification and amino acid sequence of rubredoxin from the hyperthermophilic archaebacterium *Pyrococcus furiosus* and secondary structure of the zinc adduct by NMR. *Biochemistry 30*, 10885–10895.

Braun, W., Vašák, M., Robbins, A.H., Stout, C.D., Wagner, G., Kägi, J.H.R., & Wüthrich, K. (1992). Comparison of the NMR solution structure and the X-ray crystal structure of rat metallothionein-2. *Proc. Natl. Acad. Sci. USA 89*, 10124–10128.

Bruschi, M. (1976). The amino acid sequence of rubredoxin from the sulphate reducing bacterium, *Desulfovibrio gigas*. *Biochem. Biophys. Res. Commun. 70*, 615–621.

Bystrov, V.F. (1976). Spin–spin coupling and the conformational states of peptide systems. *Prog. NMR Spectrosc. 10*, 41–81.

Carson, G.K., Dean, P.A., & Stillman, M.J. (1981). A multinuclear (^{1}H, ^{13}C, ^{113}Cd) nuclear magnetic resonance and magnetic circular dichroism spectroscopic study of thiolate complexes of cadmium. *Inorg. Chim. Acta 56*, 59–71.

Donato, H., Mani, R.S., & Kay, C.M. (1991). Spectral studies on cadmium ion binding properties of bovine brain S-100b protein. *Biochem. J. 276*, 13–18.

Frankel, A.D., Bredt, D.S., & Pabo, C.O. (1988). Tat protein from human immunodeficiency virus forms a metal-linked dimer. *Science 240*, 70–73.

Frey, M., Sieker, L., Payan, F., Haser, R., Bruschi, M., Pepe, G., & LeGall, J. (1987). Rubredoxin from *Desulfovibrio gigas*: A molecular model of the oxidised form at 1.4 Å resolution. *J. Mol. Biol. 197*, 525–541.

Frey, M.H., Wagner, G., Vašák, M., Sørensen, O.W., Neuhaus, D., Wörgötter, E., Kägi, J.H.R., Ernst, R.R., & Wüthrich, K. (1985). Polypeptide–metal cluster connectivities in metallothionein-2 by novel ^{1}H-^{113}Cd heteronuclear two-dimensional NMR experiments. *J. Am. Chem. Soc. 107*, 6847–6851.

Gronenborn, A.M., Bax, A., Wingfield, P.T., & Clore, G.M. (1989). A powerful method of sequential proton resonance assignment in proteins using relayed ^{15}N-^{1}H multiple quantum coherence spectroscopy. *FEBS Lett. 243*, 93–98.

Gunter, J.D., Schreiner, A.F., & Evans, R.S. (1975). Study of the electronic excited states of tetrahalomercurate complex ions, $[HgX_4]^{2-}$. Magnetic circular dichroism spectroscopy and use of all-centre angular momentum matrix. *Inorg. Chem. 14*, 1589–1592.

Holmquist, B. & Vallee, B.L. (1973). Tryptophan quantitation by magnetic circular dichroism in native and modified proteins. *Biochemistry 12*, 4409–4417.

Holmquist, B. & Vallee, B.L. (1979). Metal-coordinating substrate analogues as inhibitors of metalloenzymes. *Proc. Natl. Acad. Sci. USA 76*, 6216–6220.

Jørgensen, C.K. (1970). Electron transfer spectra. *Prog. Inorg. Chem. 12*, 101–157.

Kägi, J.H.R. & Vallee, B.L. (1961). Metallothionein: A cadmium and zinc containing protein from equine renal cortex. II. Physicochemical properties. *J. Biol. Chem. 236*, 2435–2442.

Karplus, M. (1959). Contact electron-spin coupling of nuclear magnetic moments. *J. Chem. Phys. 30*, 11–15.

Live, D., Armitage, I.M., Dalgarno, D.C., & Cowburn, D. (1985a). Two-dimensional ^{1}H-^{113}Cd chemical-shift correlation maps by ^{1}H-detected multiple-quantum NMR in metal complexes and metalloproteins. *J. Am. Chem. Soc. 107*, 1775–1777.

Live, D.H., Kojiro, C.L., Cowburn, D., & Markley, J.L. (1985b). Identification of proton NMR signals from the metal ligands of cadmium-substituted plastocyanin via two-dimensional multiple-quantum detection in the absence of explicitly resolved ^{1}H-^{113}Cd coupling. *J. Am. Chem. Soc. 107*, 3043–3045.

Marion, D., Driscoll, P.C., Kay, L.E., Wingfield, P.T., Bax, A., Gronenborn, A.M., & Clore, G.M. (1989). Overcoming the overlap problem in the assignment of ^{1}H NMR spectra of larger proteins by use of three-dimensional heteronuclear ^{1}H-^{15}N Hartmann-Hahn-multiple quantum coherence and nuclear Overhauser-multiple quantum coherence spectroscopy: Application to interleukin 1β. *Biochemistry 28*, 6150–6156.

McMillin, D.R. (1978). The origin of the intense absorption of azurin. *Bioinorg. Chem. 8*, 179–184.

Moura, L., Bruschi, M., LeGall, J., Moura, J.J.G., & Xavier, A.V. (1977). Isolation and characterization of desulforedoxin, a new type of non-heme iron protein from *Desulfovibrio gigas*. *Biochem. Biophys. Res. Commun. 75*, 1037–1044.

Moura, I., Teixeira, M., LeGall, J., & Moura, J.J.G. (1991). Spectroscopic studies of cobalt and nickel substituted rubredoxin and desulforedoxin. *J. Inorg. Biochem. 44*, 127–139.

Otvos, J.D., Engeseth, H.R., & Wehrli, S. (1985). Multiple-quantum ^{113}Cd-^{1}H correlation spectroscopy as a probe of metal coordination environments in metalloproteins. *J. Magn. Reson. 61*, 579–584.

Pan, T.P., Freedman, L.P., & Coleman, J.E. (1990). Cadmium-113 NMR studies of the DNA binding domain of the mammalian glucocorticoid receptor. *Biochemistry 29*, 9218–9225.

Summers, M.F. (1988). ^{113}Cd NMR spectroscopy of coordination compounds and proteins. *Coord. Chem. Rev. 86*, 43–134.

Sytkowski, A.J. & Vallee, B.L. (1979). Cadmium-109 as a probe of the metal binding sites in horse liver alcohol dehydrogenase. *Biochemistry 18*, 4095–4099.

Vašák, M., Kägi, J.H.R., & Hill, H.A.O. (1981). Zinc(II), cadium(II), and mercury(II) thiolate transitions in metallothionein. *Biochemistry 20*, 2852–2856.

Willner, H., Vašák, M., & Kägi, J.H.R. (1987). Cadmium-thiolate clusters in metallothionein: Spectrophotometric and spectropolarimetric features. *Biochemistry 26*, 6287–6292.

Wüthrich, K. (1986). *NMR of Proteins and Nucleic Acids*. John Wiley & Sons, New York.